Pharmaceutical Sciences, 2024, 30(4), 469-477
doi:10.34172/PS.2024.21
https://ps.tbzmed.ac.ir/

Research Article

In Situ Hydrogel-Forming Powders Containing Eutectic Mixture of Curcumin-Arginine as a Multi-Drug Delivery System for Wound Healing Applications

Faranak Ghaderi[1], Saeed Fathyounes[2], Shahram Emami[3*]

[1]*Department of Food and Pharmaceutical Control, School of Pharmacy, Urmia University of Medical Sciences, Urmia, Iran.*
[2]*Student Research Committee, School of Pharmacy, Urmia University of Medical Sciences, Urmia, Iran.*
[3]*Department of Pharmaceutics, School of Pharmacy, Urmia University of Medical Sciences, Urmia, Iran.*

Article Info

Article History:
Received: 6 May 2024
Accepted: 2 Jul 2024
ePublished: 24 Jul 2024

Keywords:
-Arginine
-Curcumin
-Eutectic mixture
-Sodium carboxy methyl cellulose
-Powder
-Hydrogel

Abstract

Background: Curcumin (CUR) has antimicrobial, anti-inflammatory, and antioxidant bioactivities and is a promising molecule to treat chronic wounds. However, CUR shows limited oral bioavailability due to low aqueous solubility and dissolution, chemical instability, and rapid metabolism in the gastrointestinal tract and liver. Therefore, topical delivery seems to provide therapeutic concentrations of CUR in a controlled manner. Arginine (ARG) promotes the wound healing process. CUR and ARG form a eutectic mixture (EMCA) that can be used for simultaneous improvement of dissolution of CUR and combinational wound therapy. Here, we have formulated in situ hydrogel-forming powders of EMCA using hydrophilic carriers.

Methods: EMCA was prepared by liquid-assisted grinding and analyzed by powder X-ray diffraction (PXRD) and Fourier transform infrared (FT-IR) methods. The formulations were prepared by mixing EMCA with sodium carboxy methyl cellulose, sodium alginate, and polyethylene glycol. Optical microscopy, flow property, dissolution rate, water uptake, hydrogel forming ability, release profile, and antioxidant activity of the formulated powders were measured and compared with raw CUR.

Results: The solid-state analyses revealed the formation of EMCA. Photographs showed that EMCA exhibited a lower particle size than raw CUR and ARG. The formulation content significantly affected fluid uptake, hydrogel-forming ability, and dissolution rate. The optimized formulation (FEP5) showed a considerable enhancement in the dissolution rate of CUR and could control the release. FEP5 also demonstrated promising characteristics including high fluid uptake and suitable hydrogel-forming ability. FEP5 enhanced the antioxidant activity of CUR from 9% to 50%. Additionally, FEP5 exhibited improved flow properties compared to raw CUR, which is crucial for practical applications in wound therapy.

Conclusion: Current work highlighted the potential of EMCA formulated as a hydrogel-forming powder as a novel formulation with improved dissolution, rapid fluid uptake, inexpensive components, feasible method of preparation, and easy application and removal for combinational wound therapy.

Introduction

Curcumin (CUR) is a hydrophobic polyphenolic compound extracted from the rhizomes of Curcuma longa.[1] CUR has shown considerable antimicrobial, anti-inflammatory, and antioxidant bioactivities, introducing it a promising candidate therapeutic molecule to treat chronic wounds with impaired healing.[2,3] However, CUR shows limited oral bioavailability due to very low aqueous solubility and dissolution, chemical instability, and rapid metabolism in the gastrointestinal tract and liver.[4] Therefore, topical delivery to wound site seems to provide therapeutic concentrations of CUR in a controlled manner. Until now several formulation approaches have been developed for this purpose such as sponges,[5] nanofibers,[6] nanoparticles,[7] and hydrogels.[8] Recently in situ hydrogel-forming powders have attracted increasing attention for wound delivery of therapeutic agents.[9] Powder formulations display better physicochemical and microbial stability than liquid or semisolid forms such as ready-to-use hydrogels.[10] These particulate systems have a simple method of use and easy removal and provide a high surface area for rapid contact between formulation components and wound fluids.[11]

*Corresponding Author: Shahram Emami, E-mail: emami.sh@umsu.ac.ir

Another advantage is applicability of powders for deep or irregular shaped wounds.[12] These powders rapidly absorb fluids from wound bed and transform to hydrogels. The formed hydrogel keeps the wound surface moist, exchanges gases, and controls the release of loaded agents.[13]

L-Arginine (ARG) is an essential amino acid with several functions in physiological processes such as cell division, immune function, and hormone release.[14] Specifically, its critical roles in the various stages of wound healing have been recognized for many years.[15] ARG promotes wound healing by two main pathways. First, it is metabolized to proline which is a necessary precursor for collagen synthesis. Second, it is a substrate for producing nitric oxide, which facilitates epithelialization, vascularization, and immune response.[16] Other beneficial activities of arginine include antibacterial[17] and antioxidant properties.[18] ARG has been loaded to hydrogels,[19] sponges,[20] and nanofibers[21] with the aim of direct and controllable delivery to the wound site.

A eutectic mixture is formed by dispersing fine particles of a crystalline drug in other crystalline coformer.[22] The components of a eutectic mixture are completely miscible in their melted form but their solid forms crystallize as separate phases, resulting in a lower melting point for the eutectic form compared to the components.[23] When a water insoluble drug forms a eutectic mixture with a hydrophilic coformer, its dissolution properties are improved because of higher surface area, better wettability, and improved solubility.[24] Conventionally, eutectic mixtures are prepared by neat grinding or liquid-assisted grinding.[25] The advantageous properties of eutectic mixtures include simple, cost effective, and scalable method of preparation and their high physical and chemical stability.[25] Furthermore, drug-drug eutectics mixtures can be developed to simultaneous improvement of dissolution properties and combinational therapy.[26] An interesting case of drug-drug eutectic systems with potential applications in wound therapy is eutectic mixture of CUR with ARG (EMCA). Gunnam and Nangia has prepared and characterized EMCA at a 1:1 ratio using solvent assisted grinding.[27] They showed that EMCA could improve the intrinsic dissolution rate and solubility of CUR by 9 and 30 times, respectively.

In the current work, we have formulated in situ hydrogel-forming powders of EMCA using hydrophilic hydrogel forming carriers. Solid-state characteristics, flow property, dissolution rate, water uptake, hydrogel forming ability, release profile, and antioxidant activity of the formulated powders were evaluated to develop a formulation with desired properties. To the best of our knowledge, this work is the first study that reports using a drug-drug eutectic mixture with the purpose of improving dissolution and combinational delivery for wound healing.

Methods

Materials

Sodium carboxy methyl cellulose (CMC) (Mw= 90 kDa) and polyethylene glycol 4000 (PEG 4000) were from Merck. Sodium alginate (SA) (medium viscosity), arginine (ARG), and raw curcumin (RCUR) were purchased from Sigma Aldrich. Any other utilized materials were analytical grade.

Preparation of CUR-ARG eutectic mixture and formulated powders

The eutectic mixture of CUR and ARG (EMCA) was prepared by the liquid-assisted grinding method described by Gunnam and Nangia.[27] A 1:1 stoichiometric ratio of CUR and ARG were ground using a mortar and pestle for 30 min with dropwise addition of 0.5 ml acetonitrile. The obtained product was dried at ambient condition overnight. The powder formulations were prepared by mixing EMCA with other components based on the ratios of Table 1 for 5 min using a pestle and mortar.

Powder X-ray diffraction (PXRD)

The XRD patterns of ARG, CUR, and EMCA were recorded using Tongda TD-3700 X-ray diffractometer over an angular range of 10–40° (2θ). The measurement conditions were 30 kV, 20 mA, step size of 0.02°, and scan rate of 2° /min.

Fourier Transform Infrared (FT-IR)

A Perkin Elmer FTIR was used to acquire FTIR spectra of ARG, CUR, and EMCA in the range of 4000 to 450 cm^{-1}. Each powder sample was blended with potassium bromide at a 1:100 ratio (w/w) and converted into a transparent disc. The spectra were collected at a resolution of 4 cm^{-1}, and scan numbers of 32.

Fluid uptake

The water absorption properties of prepared formulations were measured using the Franz diffusion cell setup.[11] The powder sample with a weight of 40 mg was placed as a layer over a cellulose membrane in the donor section with a surface area of 1.77 cm^2. Deionized water was filled in the receiver section, and the setup temperature was maintained at 32°C. Water absorption by the powder sample led to a lowered water level in the receiver section. At time points of 5, 15, 45, 90, 120, and 180 min, the volume of water that was needed to return the receiver volume to the starting level was measured. The fluid uptake (%) was calculated using the following equation:

$$Fluid\ uptake\ (\%) = \frac{\rho V_t}{W_p} \times 100$$

Table 1. The components and their ratios (w/w) used for different formulated powders.

Formulations	EMCA	SA	PEG	CMC
FEP1	0.5	4	-	-
FEP2	0.5	2	2	-
FEP3	0.5	1	2	1
FEP4	0.5		2	2
FEP5	0.5	-	-	4

Where ρ, V_t, and W_p were the density of water (1 g/cm^3), the measured volume at time 't', and powder weight, respectively.

Hydrogel mechanical integrity

To evaluate viscosity and mechanical strength of formed hydrogels, 40 mg of each powder formulation was mixed with 1 ml of phosphate buffer (pH 7.4) in a glass vial and the first photograph was taken after allowing to stand for 30 s. Then the vial was inverted and the second photograph was captured after 15 s.

In vitro dissolution studies

The dissolution tests were conducted using a USP apparatus 2 dissolution tester (Pharma Test co, Germany) for RCUR, EMCA, and Formulated powders. The experiments were performed using powder samples equivalent to 10 mg of CUR, 100 mL ethanol 40% (v/v) as dissolution medium, paddle speed of 100 rpm, and a temperature of 32 ± 0.5 °C. Aliquots of 5 ml were collected at 10, 20, 30, 60, 90, and 120 min and replaced with fresh ethanolic solution to prevent volume change. The concentration of CUR in collected samples was determined at 430 nm utilizing a Cecil UV-visible spectrophotometer.

Optical microscopy

An Oxion optical microscope was used to produce the images of powder samples. For this purpose, aliquots of powder samples were suspended in the silicon oil, and their photographs were taken by a digital camera at a magnification of × 40, applying Image focus alpha software.

Bulk and tapped density

Density measurements were performed by a glass syringe as described elsewhere.[28] Briefly, the volume and weight of each powder sample filled in a 1 ml syringe were measured to calculate bulk density. In the next step, the syringe was tapped repeatedly on a hard surface to a constant volume and tapped density was determined as the ratio of the powder weight to the tapped volume. The Hausner ratio was the ratio of tapped density to bulk density.

In vitro release studies

Measuring in vitro release of a hydrogel by Franz cell apparatus can reflect in vivo release behavior where this formulation is in contact with the wound bed by only one surface.[29] A dialysis membrane with a cut-off value of 14 kDa and surface area of 1.77 cm^2 was fixed between donor and receiver parts. The optimized formulation (FEP5) was mixed with deionized water at a ratio of 1:50 (w/w), and one gram of the formed hydrogel (containing 6.36 mg CUR) was spread over the donor part. As the comparison, the release experiment was also conducted for CUR powder (5 mg) dispersed in 1 ml of water. The reservoir medium was 40 %v/v ethanol stirred at 750 rpm by a magnetic stirrer. The temperature of the setup was maintained at 32 ± 1°C. Aliquots of 1 ml were sampled at selected time points and refilled with fresh ethanolic solution to prevent volume change. The concentration of CUR in the samples was determined at 430 nm employing a Cecil UV–vis Spectrophotometer. The release flux was calculated by dividing the slope of release profile to exposed surface area.

In vitro antioxidant assay

The antioxidant activities of RCUR, ARG, EMCA, and FEP5 were evaluated using 2,2-diphenyl-1-picrylhydrazyl (DPPH) radical scavenging method.[30] First, DPPH solution with the concentration of 36 µM was prepared in methanol. In the next step, ~2 mg of RCUR, ~1 mg of ARG, ~3 mg of EMCA, and ~27 mg of FEP5 were dissolved in 5 ml of phosphate buffer (pH 7.4) and then centrifuged at 12500 rpm for 10 min to precipitate undissolved CUR. Then 1 ml of each sample were added to 1ml of DPPH solution, mixed and allowed to stand in a dark place at room temperature. After 30 min of storage, the absorbance of test solutions was determined at 517 nm using a Cecil UV–vis Spectrophotometer. The absorbance of a solution of phosphate buffer mixed with DPPH solution in a 1:1 (v/v) ratio was used as the blank. DPPH inhibition (%) was calculated using the following formula:

$$DPPH\ inhibition\ (\%) = \frac{(Abs_{control} - Abs_{test})}{Abs_{control}} \times 100$$

where $Abs_{control}$ and Abs_{test} are absorbance values of blank solution and test solution, respectively. The statistical analysis of the obtained data was conducted by GraphPad Prism software with one-way analysis of variance (ANOVA) followed by the post hoc Tukey's test.

Results and Discussion

In the upcoming sections, we first characterize prepared EMCA by PXRD and FTIR methods. Then fluid uptake, hydrogel forming ability, and dissolution properties of the prepared formulations are evaluated to select best formulation. Finally, release profile, flow property, and antioxidant activity of the optimized formulation is compared with RCUR.

PXRD

Crystalline phases of untreated powders and eutectic components can be studied by PXRD. Figure 1 presents PXRD patterns of RCUR, ARG, and EMCA. RCUR was a crystalline material with sharp peaks at 2θ values of 12.3, 14.6, 15.9, 17.4, 18.3, 19.8, 19.6, 21.4, 23.5, 23.9, 24.7, 25.7, 26.2, 27.5, and 29.1. These characteristic peaks matched with the crystal form I of CUR.[31] ARG displayed its distinctive peaks at 2θ values of 11, 16.9, 18.2, 19.4, 23, and 27.4°.[32] The PXRD pattern of EMCA had the characteristic peaks of both crystalline CUR and ARG without any new peak and change in peak position. However, a small background halo pattern, peak broadening, and reduced intensity were observed in the EMCA pattern (Figure 1C), suggesting that the applied liquid-assisted co-grinding

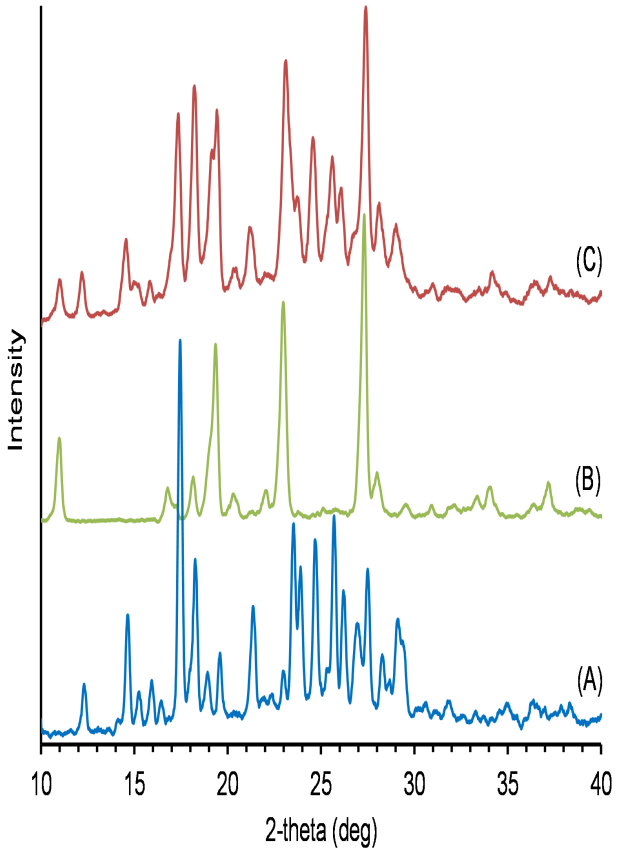

Figure 1. Overlay of PXRD patterns of RCUR (A), ARG (B), and EMCA (C).

technique produced a minor amount of amorphous phase.[23] To conclude, PXRD experiments confirmed that EMCA contains separate crystalline phases of ARG and CUR and ruled out the presence of any new crystalline phase.

FTIR

FTIR spectra of ARG, RCUR, and EMCA were recorded to evaluate their chemical structures and possible chemical interactions between ARG and CUR introduced by eutectic formation (Figure 2). The appearance of new absorptions or significant shifts in the absorptions in the FT-IR spectrum shows intermolecular interactions or chemical modifications.[25] In Figure 2, we have also provided the chemical structures of ARG and CUR along with their main characteristic FTIR peaks. The FTIR spectrum of ARG showed several characteristic absorptions at 3300, 1680, 1612, 1421, and 1137 cm^{-1} related to the bonds mentioned in Figure 2A in good agreement with literature.[33] On the other hand, RCUR main absorptions appeared (Figure 2B) at 3510, 1628, 1510, 1281, and 1153 cm^{-1} in correspondence with the literature.[34] In the spectrum of EMCA (Figure 2C), we could not detect new absorptions and most of the absorptions related to CUR and ARG remained unchanged in the EMCA as previously reported by Gunnam and Nangia.[27] This result ruled out any modifications in chemical structure of CUR or ARG. There are only a number of minor changes in the peak positions, such as a red shift for O–H of CUR from 3510 cm^{-1} to 3504 cm^{-1}, or blue shift C–C–N of ARG from 1137

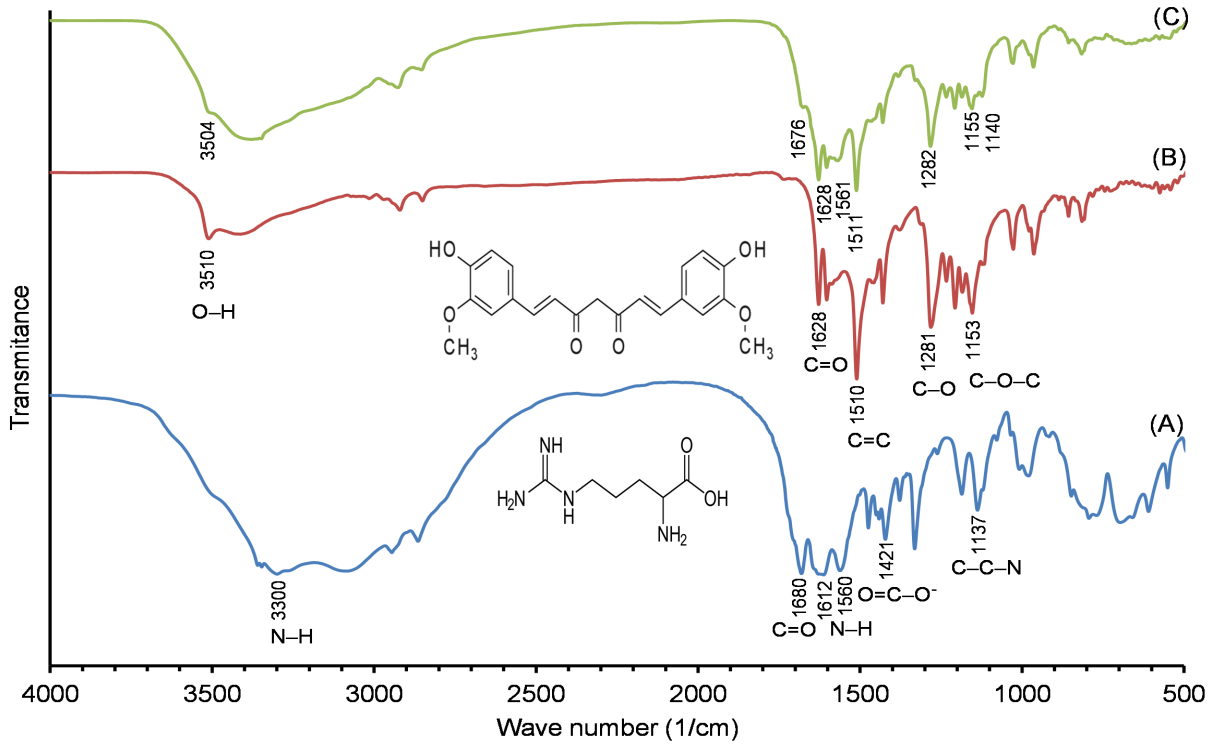

Figure 2. Overlay of FTIR records of ARG (A), RCUR (B), and EMCA (C).

cm^{-1} to 1140 cm^{-1}. However, such minor shifts cannot prove the formation of a new solid form. The lack of strong intermolecular interactions between ARG and CUR observed in FTIR experiments favored the presence of CUR and ARG as separate crystalline phases in the structure of EMCA.

Fluid uptake

A powder intended for wound delivery should rapidly absorb fluids from the wound bed and form a hydrogel to exert its dressing, wound healing, and drug release purposes.[11] In addition, the applied powder should have enough capacity to handle excess fluids secreted by exudative wounds.[35] Therefore, it is essential to investigate fluid uptake capacities of in situ hydrogel-forming powders. Figure 3 presents fluid uptake profiles of prepared formulations. It can be understood by comparing fluid uptake profiles of different formulations that the fluid uptake increased by increasing CMC content. FEP5 with higher content of CMC showed the most water absorption amounts. This formulation absorbed around 600 and 3600% of water within 15 and 180 min, respectively. It has been reported that a hydrogel-forming powder containing alginate, pectin, and polyethylene glycol could absorb around 200 and 375 % of fluid within 20 and 270 min, respectively.[36] On the other hand, De Cicco and coworkers reported that a powder composed of alginate and pectin prepared by spray drying could absorb about 1200 % fluid within 30 min.[37]

Hydrogel mechanical integrity

When a wound powder absorbs fluids, it should transform into a hydrogel with enough structural integrity and adhesiveness to the wound surface. These properties are essential to maintain formed hydrogel at the wound site, integrate it with the wound tissue, and prevent its leaking into the surrounding tissue.[38]

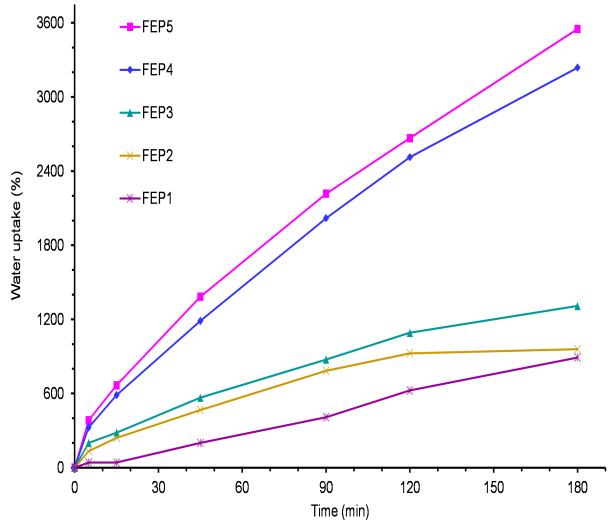

Figure 3. Water uptake profiles of prepared formulations.

To evaluate and compare the ability of the various formulated powders to form a semisolid hydrogel in situ, their appearances were observed following mixing the powders with phosphate buffer and allowing formed mixtures to flow (Figure 4). Among different formulations, FEP5 showed the highest viscosity (no movement) and FEP1 showed lowest viscosity (fluid like flow). We observed that formulations with higher CMC content had better mechanical strengths. This property is in agreement with higher water absorption of CMC based formulations as discussed in the previous section.[39] Furthermore, CMC has effective adherence to wound bed. Considering these, FEP5 can form a hydrogel with excellent residence time in the wound bed.

In vitro dissolution studies

Figure 5 shows dissolution profiles of studied powder samples. During dissolution experiments, RCUR showed negligible dissolved amount even after 120 min. As expected EMCA improved dissolution of CUR in line with the results of Gunnam and Nangia.[27] Furthermore, all prepared formulations showed higher dissolution rates than EMCA and the order of dissolution rate was as follows: FEP3>FEP5≈ FEP4≈ FEP2> FEP1> EMCA> CUR. FEP3 and FEP5 displayed about 2 times higher dissolved CUR than EMCA. These higher dissolution rates can be explained by better dispersibility and solubilizing effects of CMC, ALG, and PEG.[40]

Optical microscopy

Figure 6 presents optical microscopy images of different powder samples. It can be seen that ARG was a crystalline material with block shaped crystals and RCUR was as irregular shaped particles (Figure 6A and B). On the other hand, applied mechanical force during synthesis of EMCA by liquid-assisted grinding led to a homogeneous distribution of micronized particles (Figure 6C). CMC had a fibrous structure with smooth surfaces (Figure 6D). In the image of FEP5, EMCA particles were dispersed between CMC fibers (Figure 6E).

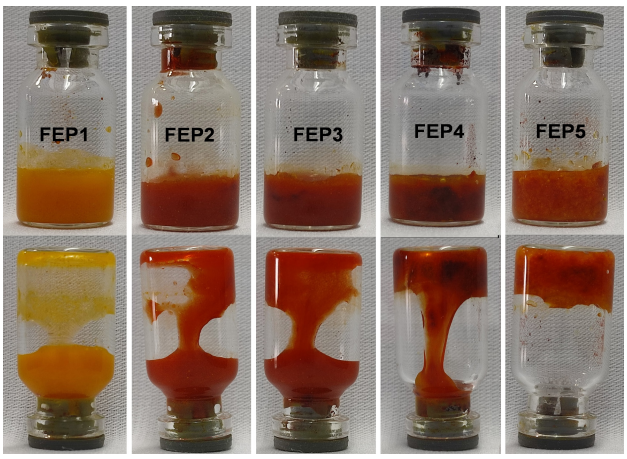

Figure 4. Photographs showing the hydrogel-forming behavior of the formulations after adding phosphate buffer to them.

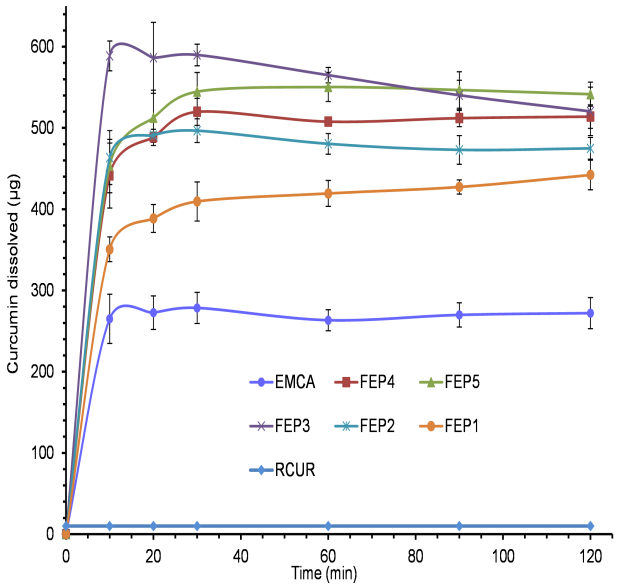

Figure 5. In vitro dissolution profiles of prepared formulations, EMCA, and RCUR.

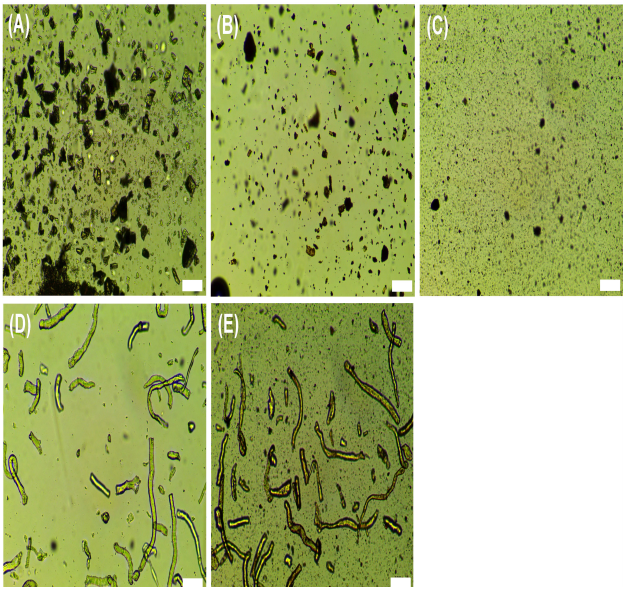

Figure 6. Optical microscopy images of ARG (A), RCUR (B), EMCA (C), CMC (D), and FEP5 (D). The scale bars indicate 100 µm.

Powder flow

Powder flow is an essential factor in the blending, handling, filling, and application of powder dosage forms.[41] Therefore, the bulk and tapped densities and Hausner ratios of RCUR, EMCA, and FEP5 were measured to evaluate the impact of prepared formulation on powder flow of RCUR (Table 2). By using Hausner ratio (HR) it is possible to classify powder samples as freely flowable or poorly flowable. Freely flowable powders exhibit HR values up to 1.25, whereas poorly flowable powders display HR values more than 1.5.[42] RCUR was a very poorly flowable powder with an HR of about 3. EMCA had better flowability than RCUR, but it still would show flow problems. On the other hand, FEP5 with a HR of 1.37 seems to be a free-flowing powder. The favorable flow properties of FEP5 enable the manufacturing of a powder dosage form with desired quality, uniform dose delivery, easy application, and uniform coverage of the wound surface.

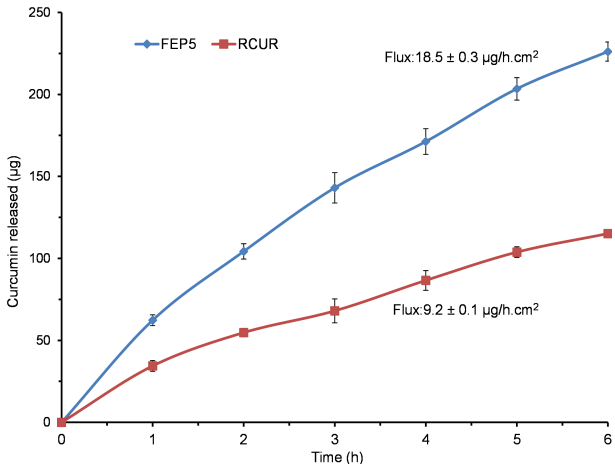

Figure 7. In vitro release profiles of FEP5 and RCUR.

Table 2. Bulk density, tapped density, and Hausner ratio of different powder samples.

Formulation	Bulk density (g/ml)	Tapped density (g/ml)	Hausner ratio
RCUR	0.30±0.01	0.68±0.04	2.99±0.14
EMCA	0.33±0.01	0.58±0.05	1.76±0.21
FEP5	0.57±0.05	0.78±0.03	1.37±0.05

In vitro release studies

Controlling the release of loaded drug to achieve desired therapeutic concentrations is a prerequisite for successful wound drug delivery.[43] Considering superior fluid uptake, good hydrogel-forming ability, and improved dissolution of FEP5, this formulation was selected for further evaluations. Figure 7 presents the release profiles of FEP5 and raw CUR. It can be seen that FEP5 released higher amounts of CUR than RCUR. The release flux for FEP5 was around two times higher than RCUR. It should be noted that although the diffusion of CUR molecules from semisolid matrix of FEP5 would be slower than liquid medium of RCUR suspension but higher concentration gradient resulted from higher solubility of EMCA led to better release profile of FEP5 compared to RCUR. This result confirmed that formulated powder can provide a controlled and sustained CUR release over 6 h.

Antioxidant activity

Phenolic hydroxyl groups of CUR are responsible for its effective antioxidant and free radical-scavenging activity.[44] In the case of ARG, the guanidinium group seems to react with free radicals and gives antioxidant activity to this amino acid.[45] DPPH free radical-scavenging assay is an easy, quick, and sensitive way to evaluate antioxidant properties of CUR.[44] Figure 8 presents DPPH assay results

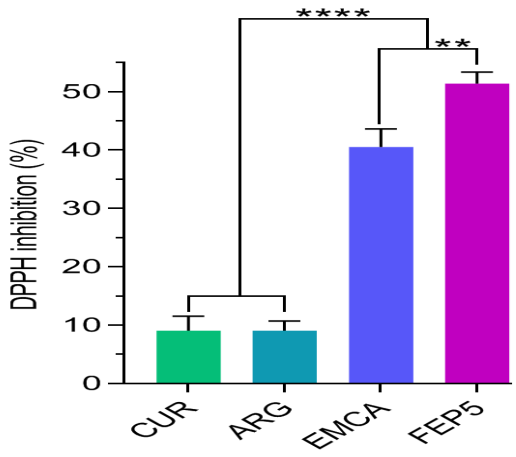

Figure 8. DPPH free-radical scavenging activities of different samples by in vitro DPPH assay (n=3, ** p< 0.0022, **** p< 0.0001).

for RCUR, ARG, EMCA, and FEP5. Both RCUR and ARG showed DPPH inhibitions of around 9%. On the other hand, EMCA could improve antioxidant activity to 40%. The highest activity was observed for FEP5 with 51% inhibition. The higher antioxidant activities of FEP5 and EMCA can be explained by their higher dissolution rates than RCUR. The previous works also indicated that CUR particles with higher dissolution rates exhibit enhanced antioxidant properties.[46,47]

Conclusion

In the current study, we have successfully prepared and characterized in situ hydrogel-forming powders for combinational delivery of CUR and ARG to the wound site. The optimized formulation, FEP5, showed a significant improvement in the dissolution rate of CUR and could provide a controlled release. FEP5 also demonstrated promising characteristics such as high fluid uptake, good hydrogel-forming ability, and enhanced antioxidant activity. Additionally, the powder formulations exhibited improved flow properties compared to RCUR, which is crucial for practical applications in wound therapy. Overall current work highlighted the great potential of drug-drug eutectic mixtures loaded in hydrogel forming powders as novel formulations with improved dissolution, inexpensive components, feasible method of preparation, easy application and removal and favorable physicochemical and microbial stability profile for designing therapeutic wound dressings.

Acknowledgments

This work was supported by the Vice Chancellor for Research and Technology of Urmia University of Medical Sciences.

Author Contributions

Faranak Ghaderi: Conceptualization, Methodology, Supervision, and Writing - Review & Editing. Saeed Fathyounes: Methodology, Investigation, Formal Analysis. Shahram Emami: Conceptualization, Funding Acquisition, Methodology, Formal Analysis, Visualization, Writing - Original Draft, Supervision.

Conflict of Interest

Dr. Shahram Emami is the associate editor of Pharmaceutical Sciences. He did not involve in peer review process of the submission. The other authors declare no conflict of interest.

References

1. Mohanty C, Das M, Sahoo SK. Emerging role of nanocarriers to increase the solubility and bioavailability of curcumin. Expert Opin Drug Deliv. 2012;9(11):1347-64. doi:10.1517/17425247.2012.724676
2. Sideek SA, El-Nassan HB, Fares AR, ElMeshad AN, Elkasabgy NA. Different curcumin-loaded delivery systems for wound healing applications: A comprehensive review. Pharmaceutics. 2023;15(1):38. doi:10.3390/pharmaceutics15010038
3. Mohanty C, Sahoo SK. Curcumin and its topical formulations for wound healing applications. Drug Discov Today. 2017;22(10):1582-92. doi:10.1016/j.drudis.2017.07.001
4. Anand P, Kunnumakkara AB, Newman RA, Aggarwal BB. Bioavailability of curcumin: Problems and promises. Mol Pharm. 2007;4(6):807-18. doi:10.1021/mp700113r
5. Dai M, Zheng X, Xu X, Kong X, Li X, Guo G, et al. Chitosan-alginate sponge: Preparation and application in curcumin delivery for dermal wound healing in rat. J Biomed Biotechnol. 2009;2009:595126. doi:10.1155/2009/595126
6. Merrell JG, McLaughlin SW, Tie L, Laurencin CT, Chen AF, Nair LS. Curcumin-loaded poly(ε-caprolactone) nanofibres: Diabetic wound dressing with anti-oxidant and anti-inflammatory properties. Clin Exp Pharmacol. 2009;36(12):1149-56. doi:10.1111/j.1440-1681.2009.05216.x
7. Krausz AE, Adler BL, Cabral V, Navati M, Doerner J, Charafeddine RA, et al. Curcumin-encapsulated nanoparticles as innovative antimicrobial and wound healing agent. Nanomed Nanotechnol Biol Med. 2015;11(1):195-206. doi:10.1016/j.nano.2014.09.004
8. Sharma A, Mittal P, Yadav A, Mishra AK, Hazari PP, Sharma RK. Sustained activity of stimuli-responsive curcumin and acemannan based hydrogel patches in wound healing. ACS Applied Bio Materials. 2022;5(2):598-609. doi:10.1021/acsabm.1c01078
9. Amante C, Falcone G, Aquino RP, Russo P, Nicolais L, Del Gaudio P. In situ hydrogel formulation for advanced wound dressing: Influence of co-solvents and functional excipient on tailored alginate–pectin–chitosan blend gelation kinetics, adhesiveness, and performance. Gels. 2024;10(1):3. doi:10.3390/

gels10010003
10. Emami S, Ebrahimi M. Bioactive wound powders as wound healing dressings and drug delivery systems. Powder Technol. 2023;423:118501. doi:10.1016/j.powtec.2023.118501
11. Romić MD, Klarić MŠ, Lovrić J, Pepić I, Cetina-Čižmek B, Filipović-Grčić J, Hafner A. Melatonin-loaded chitosan/pluronic® f127 microspheres as in situ forming hydrogel: An innovative antimicrobial wound dressing. Eur J Pharm Biopharm. 2016;107:67-79. doi:10.1016/j.ejpb.2016.06.013
12. Chen Y-W, Lu C-H, Shen M-H, Lin S-Y, Chen C-H, Chuang C-K, Ho C-C. In vitro evaluation of the hyaluronic acid/alginate composite powder for topical haemostasis and wound healing. Int Wound J. 2020;17(2):394-404. doi:10.1111/iwj.13285
13. Pagano C, Calarco P, Di Michele A, Ceccarini MR, Beccari T, Primavilla S, et al. Development of sodium carboxymethyl cellulose based polymeric microparticles for in situ hydrogel wound dressing formation. Int J Pharm. 2021;602:120606. doi:10.1016/j.ijpharm.2021.120606
14. Fu C, Qi Z, Zhao C, Kong W, Li H, Guo W, Yang X. Enhanced wound repair ability of arginine-chitosan nanocomposite membrane through the antimicrobial peptides-loaded polydopamine-modified graphene oxide. J Biol Eng. 2021;15(1):17. doi:10.1186/s13036-021-00268-3
15. Zhou Y, Liu G, Huang H, Wu J. Advances and impact of arginine-based materials in wound healing. J Mater Chem B. 2021;9(34):6738-50. doi:10.1039/D1TB00958C
16. Hussein Y, El-Fakharany EM, Kamoun EA, Loutfy SA, Amin R, Taha TH, et al. Electrospun pva/hyaluronic acid/l-arginine nanofibers for wound healing applications: Nanofibers optimization and in vitro bioevaluation. Int J Biol Macromol. 2020;164:667-76. doi:10.1016/j.ijbiomac.2020.07.126
17. Song J, Feng H, Wu M, Chen L, Xia W, Zhang W. Preparation and characterization of arginine-modified chitosan/hydroxypropyl methylcellose antibacterial film. Int J Biol Macromol. 2020;145:750-8. doi:10.1016/j.ijbiomac.2019.12.141
18. Allur Subramaniyan S, Sheet S, Balasubramaniam S, Berwin Singh SV, Rampa DR, Shanmugam S, et al. Fabrication of nanofiber coated with l-arginine via electrospinning technique: A novel nanomatrix to counter oxidative stress under crosstalk of co-cultured fibroblasts and satellite cells. Cell Commun Adhes. 2018;24(1):19-32. doi:10.1080/15419061.2018.1493107
19. Aleem AR, Shahzadi L, Tehseen S, Alvi F, Chaudhry AA, Rehman Iu, Yar M. Amino acids loaded chitosan/collagen based new membranes stimulate angiogenesis in chorioallantoic membrane assay. Int J Biol Macromol. 2019;140:401-6. doi:10.1016/j.ijbiomac.2019.08.095
20. Matsumoto Y, Kuroyanagi Y. Development of a wound dressing composed of hyaluronic acid sponge containing arginine and epidermal growth factor. J Biomater Sci Polym Ed. 2010;21(6-7):715-26. doi:10.1163/156856209X435844
21. Mirhaj M, Tavakoli M, Varshosaz J, Labbaf S, Salehi S, Talebi A, et al. Preparation of a biomimetic bi-layer chitosan wound dressing composed of a-prf/sponge layer and l-arginine/nanofiber. Carbohydr Polym. 2022;292:119648. doi:10.1016/j.carbpol.2022.119648
22. Goldberg AH, Gibaldi M, Kanig JL. Increasing dissolution rates and gastrointestinal absorption of drugs via solid solutions and eutectic mixtures i: Theoretical considerations and discussion of the literature. J Pharm Sci. 1965;54(8):1145-8. doi:10.1002/jps.2600540810
23. Fandaruff C, Quirós-Fallas MI, Vega-Baudrit JR, Navarro-Hoyos M, Lamas DG, Araya-Sibaja AM. Saquinavir-piperine eutectic mixture: Preparation, characterization, and dissolution profile. Pharmaceutics. 2023;15(10):2446. doi:10.3390/pharmaceutics15102446
24. Emami S, Siahi-Shadbad M, Barzegar-Jalali M, Adibkia K. Characterizing eutectic mixtures of gliclazide with succinic acid prepared by electrospray deposition and liquid assisted grinding methods. J Drug Deliv Sci Technol. 2018;45:101-9. doi:10.1016/j.jddst.2018.03.006
25. Bazzo GC, Pezzini BR, Stulzer HK. Eutectic mixtures as an approach to enhance solubility, dissolution rate and oral bioavailability of poorly water-soluble drugs. Int J Pharm. 2020;588:119741. doi:10.1016/j.ijpharm.2020.119741
26. Thipparaboina R, Thumuri D, Chavan R, Naidu VGM, Shastri NR. Fast dissolving drug-drug eutectics with improved compressibility and synergistic effects. Eur J Pharm Sci. 2017;104:82-9. doi: 10.1016/j.ejps.2017.03.042
27. Gunnam A, Nangia AK. Solubility improvement of curcumin with amino acids. CrystEngComm. 2021;23(18):3398-410. doi:10.1039/D1CE00171J
28. Sansone F, Aquino RP, Gaudio PD, Colombo P, Russo P. Physical characteristics and aerosol performance of naringin dry powders for pulmonary delivery prepared by spray-drying. Eur J Pharm Biopharm. 2009;72(1):206-13. doi:10.1016/j.ejpb.2008.10.007
29. Andrianopoulou A, Sokolowski K, Wenzler E, Bulman ZP, Gemeinhart RA. Assessment of antibiotic release and antibacterial efficacy from pendant glutathione hydrogels using ex vivo porcine skin. J Control Release. 2024;365:936-49. doi:10.1016/j.jconrel.2023.12.008
30. Celebioglu A, Uyar T. Fast-dissolving antioxidant curcumin/cyclodextrin inclusion complex electrospun nanofibrous webs. Food Chem. 2020;317:126397. doi:10.1016/j.foodchem.2020.126397
31. Sanphui P, Goud NR, Khandavilli UBR, Bhanoth S, Nangia A. New polymorphs of curcumin. Chem

Commun. 2011;47(17):5013-5. doi:10.1039/C1CC10204D
32. Park H, Seo HJ, Ha E-S, Hong S-h, Kim J-S, Kim M-S, Hwang S-J. Preparation and characterization of glimepiride eutectic mixture with l-arginine for improvement of dissolution rate. Int J Pharm. 2020;581:119288. doi:10.1016/j.ijpharm.2020.119288
33. Antunes BP, Moreira AF, Gaspar VM, Correia IJ. Chitosan/arginine–chitosan polymer blends for assembly of nanofibrous membranes for wound regeneration. Carbohydr Polym. 2015;130:104-12. doi:10.1016/j.carbpol.2015.04.072
34. Zhang C, Jahan SA, Zhang J, Bianchi MB, Volpe-Zanutto F, Baviskar SM, et al. Curcumin nanocrystals-in-nanofibres as a promising platform for the management of periodontal disease. Int J Pharm. 2023;648:123585. doi:10.1016/j.ijpharm.2023.123585
35. Mndlovu H, Kumar P, du Toit LC, Choonara YE. In situ forming chitosan-alginate interpolymer complex bioplatform for wound healing and regeneration. AAPS PharmSciTech. 2022;23(7):247. doi:10.1208/s12249-022-02397-4
36. Lee J, Hlaing SP, Cao J, Hasan N, Ahn H-J, Song K-W, Yoo J-W. In situ hydrogel-forming/nitric oxide-releasing wound dressing for enhanced antibacterial activity and healing in mice with infected wounds. Pharmaceutics. 2019;11(10):496. doi:10.3390/pharmaceutics11100496
37. De Cicco F, Reverchon E, Adami R, Auriemma G, Russo P, Calabrese EC, et al. In situ forming antibacterial dextran blend hydrogel for wound dressing: Saa technology vs. Spray drying. Carbohydr Polym. 2014;101:1216-24. doi:10.1016/j.carbpol.2013.10.067
38. Chen T, Chen Y, Rehman HU, Chen Z, Yang Z, Wang M, et al. Ultratough, self-healing, and tissue-adhesive hydrogel for wound dressing. ACS Appl Mater Interfaces. 2018;10(39):33523-31. doi:10.1021/acsami.8b10064
39. Mansur AAP, Rodrigues MA, Capanema NSV, Carvalho SM, Gomes DA, Mansur HS. Functionalized bioadhesion-enhanced carboxymethyl cellulose/polyvinyl alcohol hybrid hydrogels for chronic wound dressing applications. RSC Adv. 2023;13(19):13156-68. doi:10.1039/D3RA01519J
40. Rane Y, Mashru R, Sankalia M, Sankalia J. Effect of hydrophilic swellable polymers on dissolution enhancement of carbamazepine solid dispersions studied using response surface methodology. AAPS PharmSciTech. 2007;8(2):27. doi:10.1208/pt0802027
41. Blanco D, Antikainen O, Räikkönen H, Mah PT, Healy AM, Juppo AM, Yliruusi J. Image-based characterization of powder flow to predict the success of pharmaceutical minitablet manufacturing. Int J Pharm. 2020;581:119280. doi:10.1016/j.ijpharm.2020.119280
42. Ali ME, Lamprecht A. Spray freeze drying as an alternative technique for lyophilization of polymeric and lipid-based nanoparticles. Int J Pharm. 2017;516(1):170-7. doi:10.1016/j.ijpharm.2016.11.023
43. Heydari P, Zargar Kharazi A, Asgary S, Parham S. Comparing the wound healing effect of a controlled release wound dressing containing curcumin/ciprofloxacin and simvastatin/ciprofloxacin in a rat model: A preclinical study. J Biomed Mater Res A. 2022;110(2):341-52. doi:10.1002/jbm.a.37292
44. Ak T, Gülçin İ. Antioxidant and radical scavenging properties of curcumin. Chem Biol Interact. 2008;174(1):27-37. doi:10.1016/j.cbi.2008.05.003
45. Lass A, Suessenbacher A, Wölkart G, Mayer B, Brunner F. Functional and analytical evidence for scavenging of oxygen radicals by l-arginine. Mol Pharmacol. 2002;61(5):1081-8. doi:10.1124/mol.61.5.1081
46. Yen F-L, Wu T-H, Tzeng C-W, Lin L-T, Lin C-C. Curcumin nanoparticles improve the physicochemical properties of curcumin and effectively enhance its antioxidant and antihepatoma activities. J Agric Food Chem. 2010;58(12):7376-82. doi:10.1021/jf100135h
47. Kakran M, Sahoo NG, Tan IL, Li L. Preparation of nanoparticles of poorly water-soluble antioxidant curcumin by antisolvent precipitation methods. J Nanopart Res. 2012;14(3):757. doi:10.1007/s11051-012-0757-0